Investigating the slope failures at the Lou rock glacier front, French Alps

Marco Marcer, Steffen Nielsen, Charles Ribeyre, Mario Kummert, P.A Duvillard, Philippe Schoeneich, Xavier Bodin, Kim Génuite

▶ **To cite this version:**

Marco Marcer, Steffen Nielsen, Charles Ribeyre, Mario Kummert, P.A Duvillard, et al.. Investigating the slope failures at the Lou rock glacier front, French Alps. Permafrost and Periglacial Processes, 2020, 31, pp.15-30. 10.1002/ppp.2035 . hal-02414643

HAL Id: hal-02414643
https://hal.science/hal-02414643

Submitted on 21 Dec 2020

HAL is a multi-disciplinary open access archive for the deposit and dissemination of scientific research documents, whether they are published or not. The documents may come from teaching and research institutions in France or abroad, or from public or private research centers.

L'archive ouverte pluridisciplinaire **HAL**, est destinée au dépôt et à la diffusion de documents scientifiques de niveau recherche, publiés ou non, émanant des établissements d'enseignement et de recherche français ou étrangers, des laboratoires publics ou privés.

Investigating the slope failures at the Lou rock glacier front, French Alps

Marco Marcer[1,2], Steffen Ringsø Nielsen[1,3], Charles Ribeyre[1], Mario Kummert[4], Pierre-Allain Duvillard[2,5], Philippe Schoeneich[1], Xavier Bodin[2], and Kim Genuite[2]

[1]Univ. Grenoble Alpes, Institut d'Urbanisme et Géographie Alpine, PACTE, 38000 Grenoble, France

[2]Univ. Savoie Mont-Blanc, CNRS, UMR CNRS 5204, EDYTEM, 73370 Le Bourget du Lac, France.

[3]Institute for Arctic Technology, Lyngby, Denmark

[4]Department of Geosciences/Geography, University of Fribourg, Switzerland

[5]IMSRN, Parc Pré Millet - 680 Rue Aristide Bergès, Montbonnot, France

ABSTRACT

On August 14th 2015 a large debris flow initiated by the occurrence of two slope failures at the front of the Lou rock glacier flooded part of the town of Lanslevillard, France. The present study aims to understand the meteorological and geomorphological context that led to these failures. Investigations were conducted by combining meteorological data, surface movements and geophysical transects. The analysis indicates that the Lou rock glacier is directly connected to an active torrential channel and has a natural predisposition to frontal failure due to the steepness of its front. The slope failures were triggered after a heat wave followed by a three-week period of almost continuous rainfall. Water flowing on top of the permafrost table was observed in the two head scarps, suggesting that regressive erosion consecutive to this concentrated subsurface water flow triggered the failures. For one of the slides, traces of previous failures were observable on historical aerial imagery dating back to the 1950's, while the second slide corresponded to a novel event and developed on the frontal slope of a fast moving and destabilized rock glacier lobe. We also discuss the increase in local predisposition to failure related to the remarkable morphological modifications such as frontal advance and development of surface cracks associated with the lobe destabilization.

1 Introduction

The town of Lanslevillard was hit by two consecutive debris flows on August 14th 2015, at 15h30 and 16h45 (Figure 1). The debris volume that reached the town was estimated to be around 15 000 m^3, causing more than 100,000 € of damage. The debris flow was triggered in the headwaters of the Arcelle Neuve stream which reaches the Arc river valley in the western part of Lanslevillard. Before reaching the Arc river, the waters of the Arcelle Neuve stream are channelled into a pipe which passes

below the local road RD 1106 (Figure 1c). During the event, the large amount of material carried by the flow rapidly clogged the pipe, causing flooding. The overflow damaged vehicles and equipments located in the Vieux Moulin cable car station and buried a restaurant cellar under two meters of debris. At that point the flow followed the local road RD 1106 towards Les Champs, an inhabited hamlet. Using an excavator, an emergency dam was quickly created and the flow was deviated into the Arc River.

On August 15^{th} 2015, a helicopter survey carried out by the National Environmental Protection Agency (RTM) located the initiation points of the debris flows on the front of the Lou rock glacier, an active landform located in the upper part of the Arcelle Neuve watershed and which was previously unknown to the local authorities (Figures 2, 3). The initiation points consisted of two slope failures whose upper limits were defined by pronounced head scarps located near the front of the rock glacier. Water springs were observed in both head scarps, about two meters below the surface of the rock glacier (Figure 3b). On August 25^{th} 2015 an in-situ survey took place in order to observe the nature of the initiation points and the characteristics of the rock glacier. The eastern initiation point was characterized by an active water spring despite the dry period after the event. The failure was up to 15 meters wide and 20 meters long. The scarp was incised by two minor gullies, reaching a depth of 3.5 meters (Figure 3). This failure therefore presented characteristics similar to those observed in the Dirru, Gugla and Tsarmine rock glaciers (Swiss Alps[1]), and which are described as resulting from large "concentrated flow", i.e. linear regressive erosion of the sediments lying on the frontal slope due to saturation from permanent groundwater and water flow from springs. The western initiation point was characterized by a marked "U" shape with a large flat bottom surface where debris cemented by ice were observed. This flat surface was 2.5 meters below the rock glacier original surface, extending 15 meters in width and 30 meters in length (Figure 3c, d). These characteristics seemed to indicate a slightly different failure development at the western initiation point, resembling the so-called "active layer detachments" (ALD) that are commonly observed in Arctic permafrost[2–4].

Since the debris flow was triggered on a rock glacier, this event takes place in the context of periglacial hazards. In the European Alps, periglacial hazards most commonly involve high altitude rock falls and increased sediment availability in Alpine watersheds[5,6]. The aim of the present study is to propose an interpretation, from a geomorphological perspective, of the drivers that led to the frontal failures of the Lou rock glaciers on August 14^{th} 2015. The objective is also to provide original documentation on the case of a debris flow originating from the front of a rock glacier. Since the rock glacier was not being monitored at that time, this study presents a back analysis mostly based on data that was collected after the event. The underlying hypothesis is that the occurrence of slope failures was controlled by a combination of local predispositions such as the topographical setting, the internal structure and the dynamics of the landform, and a preparatory sequence leading to a trigger that can be linked to the meteorological events prior to the failures.

These hypotheses are based on previous studies investigating mass movements in permafrost terrain. For instance, the local topographical setting can be conducive to the development and propagation of debris flows due to the presence of steep slopes connecting the front of the rock glacier and the main torrential channel[7,8]. Rock glacier dynamics and stability, which are also

related to local topography[9–11], can further increase the susceptibility to frontal instabilities[12,13]. In addition, meteorological conditions can represent important predisposing and triggering factors of the failures. It has been observed that temperatures close to 0 °C reduce shear strength[14] and fracture toughness[15] of frozen materials and that heat waves have often been linked to significant mass movements in permafrost terrains[16,17]. Meteoric or meltwater infiltration has also been identified as an important preparatory and triggering factor for frontal instabilities[1,12].

Under the assumption that these external (weather related) and internal (internal structure and dynamic) factors controlled the failure occurrence, we investigated the event by analysing data describing these parameters. Meteorological and nivological data were analysed initially, in order to understand the meteorological context prior to and during the event (methods in section 3.1). Decadal-scale evolution of the surface velocity as well as the changes in the surface morphology were investigated using aerial orthomosaics, which were retrieved by historical aerial imagery and UAV surveys after the event (methods described in section 3.2). The topographical settings and geomorphological characteristics were observed in the field as well as by UAV surveys (study site described in section 2). The internal structure of the landform was inferred from the electrical resistivity tomography and seismic refraction campaign conducted in 2016 and 2017 (methods described in section 3.3). A comprehensive analysis of the data is then proposed, resulting in diagnosis of the 2015 failures (section 5.3). Finally, the legacy of this event is presented including the risk management plan adopted by the local authorities and the recommendations for future efforts on this site (section 5.4).

2 Study site

2.1 General setting

The Lou rock glacier is located in the Mont Cenis range, i.e. the orographic barrier between the Maurienne (France) and Susa (Italy) valleys. The Pointe de Ronce (3612 m a.s.l.) is one of the highest peaks in the massif (Figure 2a). Its west ridge descends to two secondary summits, the Signal du Grand Mont Cenis (3356 m a.s.l.) and the Pointe de la Nunda (3023 m a.s.l.) located further to the west. The north face of the saddle separating these two minor summits (Col du Lou, 3040 m a.s.l.) contains the zone of origin of the Lou rock glacier, which develops on a ledge in the topography at 2700 m a.s.l..

The Mont Cenis range is part of the Piemont-Liguria Penninic nappe, consisting of Cretaceous Bunder-schists ophiolites[18]. In the north face of the Signal du Gran Mont Cenis where the rock glacier is located, two stratigraphic series can be identified. From the valley bottom to 2600 m a.s.l. calcschists and marbles are found, while the mountain summit is made up of phyllite marbles. In addition, black schists can be observed above 3400 m a.s.l. on the highest summits of the range. All these series are densely jointed and prone to mechanical weathering, as can be seen in the many scree slopes and late Würm glacial deposits in the area[18].

The area presents the typical traits of the dry climate that characterizes the eastern side of the Northern French Alps[19]. The 0°C isotherm (second half of the 20^{th} century) is located at 2600 m a.s.l. while mean annual precipitation at the valley bottom is of the order of 800 mm/y[19,20]. Glaciers can be found only in the form of small ice aprons perched on the north faces of

the highest summits and cover in total about 2.5 km^2, extending from 3000 to 3500 m a.s.l. (data from 2009[21]). Conditions favourable to the existence of permafrost are expected to be found above 2500 m a.s.l. on north faces and above 2900 m a.s.l. on south slopes[22]. HISTALP data

Surface sediment transport is mainly dominated by gravitational (rock falls) and torrential processes (gullying, debris flows), and numerous gullies and couloirs can be observed on steep slopes on all aspects. Although the periglacial environment is extensive in the region[22,23], the Signal du Gran Mont Cenis area contains only a few rock glaciers due to the rareness of flat surfaces where rock debris can accumulate. One of the few ledges is the site of the Lou rock glacier, which has a surface of about 0.2 km^2 and is characterized by the presence of several fronts overhanging the steep gullies (>40°), which correspond to the headwaters of the Arcelle Neuve stream where the 2015 debris flow took place.

2.2 The Lou rock glacier

The Lou rock glacier can be defined as "pebbly"[24] as the largest clast size observed at the surface is of the order of a few decimeters. Instead of the typical single tongue and single front shape, the Lou rock glacier has five frontal lobes surrounding the gullies in cirque-type configuration with steep frontal slopes ranging between 38°and 42°(Figure 2b). The landform can thus be defined also as a polymorphic rock glacier[25]. Due to this complex morphology, the specific toponomy presented in Figure 2c will be used throughout the paper.

Two main frontal lobes separated by an embankment that bends eastwards characterize the eastern and central part of the rock glacier. These eastern and central lobes flow downslope from a plateau which receives a supply of debris from the scree slope leading to the Col du Lou pass. While the central part of this plateau is relatively flat, the eastern side presents a clear depression, suggesting the past presence of a small glacier. The embankment that separates the central and eastern part of the plateau can be interpreted as the lateral moraine of this glacier. The easternmost slope failure related to the occurrence of the 2015 debris flows, i.e. the eastern slide, developed where this lateral moraine reaches the front line and leans over the gully.

The western side of the rock glacier complex is characterized by three lobes which are supplied directly by the surrounding headwalls. While the two westernmost lobes (inactive lobes in Figure 2c), are partially vegetated and present a rounded topography, the third lobe shows clear signs of intense activity. This lobe is characterized by a dense network of cracks that scar the surface every 2 – 5 meters. The cracks are shallow, measuring up to 20 meters long and 1-2 meters deep and wide, and create a rugged microtopography with "steps" on the surface, measuring one to two meters in height and width (Figure 4). None of the cracks cut the lobe through its entire thickness, but rather disconnect it from the two adjacent lobes (inactive lobes and central lobe). These characteristics are typical of pebbly rock glaciers showing signs of destabilization[11]. The western slide associated with the 2015 debris flow events occurred on the orographic right-hand side of this western lobe's front.

3 Methods

3.1 Meteorological data

Meteorological conditions prior to the event were investigated by analysing air temperature, rainfall and snow cover data relative to the 2014-2015 winter season and the summer of 2015. Meteorological anomalies were also investigated by comparing the 2014-2015 data with the average and typical variability of the available time series.

The main meteorological data (air temperature and precipitation) were obtained from the Mont Cenis weather station located at 2035 m a.s.l., 3 km away from the site (station id: 73144001, Figure 2a). The station is property of Météo-France and has recorded daily mean air temperature and precipitation since 1992. In addition, data from the Bessans weather station located at 1710 m a.s.l. and 7 km north-east from the site (station id: 73040005) was used to fill the gaps in the data series from the Mont Cenis station. The procedure to fill these gaps was carried out by looking at the correlation between data for periods during which both stations provided continuous measurements and applying the linear regression model to predict missing data at Mont Cenis.

The Bessans weather station also provided snow height data series for a period spanning from winter 2011-2012 to 2017. Since snow height values were acquired every 1 to 4 days, the resulting database is discontinuous and only suitable for qualitative analysis.

3.2 Dynamical behaviour

The spatio-temporal evolution of permafrost creep velocities that characterize the rock glacier was investigated in order to understand its past and current dynamics. First, the observation of time series of orthoimages allowed the evolution of the rock glacier surface velocities over the past decades to be reconstructed at coarse temporal resolution, i.e. velocity averaged over several years[26,27]. Differential GPS (dGPS) surveys have then been performed at least once a year since 2015 to quantify the annual displacements of a few points to a high degree of precision[28]. Finally, UAV imagery was acquired in 2016, 2017 and 2018 to compute and compare high-resolution orthophotos and Digital Elevation Models (DEMs) to understand the deformation pattern and the spatial characteristics of erosion-deposition on the destabilized lobe[13,29]. UAV surveys were preferred to terrestrial radar and laser scanning[12,30] because of the lack of suitable viewpoints to set up instruments near the Lou rock glacier.

3.2.1 Historical aerial imagery

Historical aerial imagery was used to reconstruct the dynamic behaviour of the rock glacier in the second half of the twentieth century. For that purpose, several orthoimages acquired at different dates were computed by triangulating aerial images and generating the DEMs using the Ortho Engine module in PCI Geomatica[26]. The raw aerial images used in this study were directly obtained from the Institut Géographique National (IGN) website where they are freely available. Distortion coefficients and focal lengths were provided by the IGN support team for the requested missions. Images from 1970 and 1996 were selected for the analysis because of the absence of features such as snow patches and shadows that may significantly reduce the precision

of the velocity estimation. In addition, already orthorectified aerial images from 2006 and 2013 (resolutions of 1 and 0.5 metersrespectively) were made available by the IGN[31] and could also be used in this study.

In order to infer surface velocity values, the selected orthoimages were compared with each other on the QGIS software. Noticeable boulders were tracked between pairs of orthoimages and their displacement rate was computed by dividing the measured displacement by the time elapsed between the two images. The uncertainty caused by image distortions and errors was quantified by tracking apparent movements on 53 non-moving areas (i.e. areas of vegetation and bedrock) uniformly distributed around the landform and averaging their value.

3.2.2 DGPS surveys

DGPS surveys were conducted using a rapid-static approach, which consists of post treating data acquired using a mobile receiver jointly with data acquired using a base station of known coordinates. This method allowed high precision (2 cm) to be reached with low acquisition time (30 seconds to 5 minutes per point, depending on satellite configuration). A Trimble Geo7x antenna combined with a TopCon (GB 1000) receiver was used as a basis. Firstly, four targets were marked and their positions measured on August 25^{th} 2015. The targets consisted of crosses made of red and green paint on several large visible boulders located on the surface of the western destabilized rock glacier lobe. Coordinates of the targets were measured again on 19^{th} July 2016 and 14^{th} September 2016 with a mobile receiver and new targets (17 in total) were added to increase spatial resolution. Surveys were then repeated on August 12^{th} 2017 and August 22^{nd} 2018. Data were treated using the software Trimble Pathfinder.

3.2.3 UAV surveys

UAV surveys were used to acquire close-range high-resolution aerial images of the destabilized lobe. The UAV-borne photogrammetric surveys were systematically performed on the same dates as the dGPS surveys (14^{th} September 2016, 12^{th} August 2017 and 22^{nd} August 2018). The 2016 mission was performed using a DJI Phantom 3, flying in manual mode. Pictures were captured at different heights, ranging from 20m to 90m above the surface. Eight targets were measured by dGPS and used as Ground Control Points (GCPs). The 2017 and 2018 surveys were performed using a DJI Mavic Pro. Surveys were carried out using an automatic flight planner, i.e. the Drone Map software. Pictures were taken at 70 to 150 m altitude and 9 (in 2017) to 12 (in 2018) GCPs were also acquired by dGPS for these campaigns.

UAV images were processed using Agisoft Photoscan following a Structure from Motion approach in order to obtain DEMs and Orthoimages[32]. Firstly, point clouds were computed using the UAV on-board GPS data to facilitate the structure reconstruction. In a second stage, GCPs were used to georeference the models. The locations of GCPs in the aerial images was manually adjusted in order to optimize the model until errors were below the pixel size[32]. Point clouds were then densified, meshed and exported as Orthoimages and DEMs.

The resulting orthoimages were downsampled at a resolution of 25 cm x 25 cm and used to estimate displacements using the module of automatic feature tracking IMCORR[33]. Unfortunately, the orthoimage obtained from the 2016 UAV survey had to be discarded for displacement estimation due to an insufficient coverage of the Eastern rock glacier lobe. As a consequence, only

the orthoimages from 2017 and 2018 were selected to perform the feature tracking analysis. Results were manually cleaned to avoid single points of both high speed and movements characterized by unrealistic direction in comparison to the general slope aspect. Correlation points were interpolated using a kriging algorithm to produce a heatmap of displacement over the rock glacier surface for the 2017-2018 time interval. The accuracy of the result was evaluated by (i) comparing the computed displacement with movements obtained from dGPS surveys and (ii) by comparing apparent movements on stable areas.

Finally, DEMs were also compared to observe surface elevation changes on the destabilized western lobe. In order to have a more precise evaluation of the surface height variations, the models were co-registered relative to the 2016 model, which had high quality on this lobe, by matching stable areas in the best fit ICP algorithm[34] in the CloudCompare software[35].

3.3 Geophysical surveys

Electrical Resistivity Tomography (ERT) and seismic refraction tomography (SRT) campaigns were performed in 2016 and 2017 to investigate the internal structure of the landform. These methods are largely used in mountain permafrost investigations to visualize the vertical transition from unfrozen to frozen ice-rich sediments using ERT[36,37] and the thickness of the different horizontal layers using SRT[38].

3.3.1 Electrical Resistivity Tomography

Two profiles of 64 electrodes (2.5 meters spacing) were acquired on September 15^{th} 2016 on the main plateau (medial and eastern plateau in Figure 2c) of the rock glacier (PE1 and PE2, Table 1). On August 10^{th} 2017, two profiles consisting of 64 electrodes (5 meters spacing) were acquired longitudinally (PE5) and transversally (PE6) on the destabilized lobe, from the foot of the front up to the rooting zone and between the two debris flow slides respectively. The acquisitions were performed using the Wenner array and the resulting data were inverted using the Res2Dinv software[39]. The positions of the electrodes were measured by dGPS Trimble Go7x and used to compute the topography of profiles.

3.3.2 Seismic Refraction

Seismic refraction was conducted using a Sesitronix DaqLink III and 24 geophone cables with 5 meters spacing. Real time connection between the Vscope software and the seismograph was ensured by Ethernet cable. Wave source was triggered by hammer hits and for each geophone 2 to 5 triggers were shot in order to achieve a clean signal. Two offset triggers were shot at a distance of 5 and 10 meters from the beginning and end of each profile. The survey took place on the western destabilized lobe on October 18^{th} 2017. In order to cover the whole length of the lobe, three seismic profiles were measured longitudinally, each of them overlapping the previous one by 6 geophones to ensure consistent transition between the different profiles.

Data was then processed using the ReflexW software. First arrivals were selected manually and checked using the automatic travel time analysis and the inversion was performed on an initial model consisting of a surface velocity of 400 m/s increasing with depth at a rate of 300 m/s/m. Surface topography was retrieved from in-situ dGPS measurements.

4 Results

4.1 Meteorological conditions prior to the event

The meteorological data from the Mont Cenis weather station during the hydrological year 2014 - 2015 presented two main gaps, respectively between November and January, and between April and June (Figure 5a,b). Data issued from the Bessans weather station were found to correlate well with Mont Cenis temperature data (R^2=0.96) allowing a robust gap filling, while correlation was weaker for precipitation data (R^2=0.61).

The winter of 2014-2015 was characterized by notably low amounts of snow accumulation (8^{th} lowest amount since 1959). In particular, November, April and May received about 80% less snow than the average since 1959[40]. December was also characterized by very little snow precipitation and very thin snow cover (Figure 5c). Temperatures oscillated from abnormally warm at the end of November (3 to 5°C than average on record) to abnormally cold in late December (-5 to -7°C than average on record). Consistent snowfalls arrived in mid-January, as the measured snow height increased from 0.2 m to 0.7 m in the Bessans weather station. However, the snow cover remained relatively thin throughout the whole winter and early spring compared to previous and following years, with snow cover approximately 0.5 m thinner than average at the peak of the accumulation season (late March).

Spring 2015 was characterized by warm temperatures in April – May, occasionally 3-5 °C higher than average. The more intense precipitation event recorded in 2015 reached 50 mm/day and was registered in mid-May at the Mont Cenis station. Given the low temperatures measured at 2000 m on this occasion, this event resulted possibly in solid precipitations at the Lou rock glacier. Temperatures increased steadily through June and then July, with an exception for an episode of rain occurring in mid-June associated with a temporary temperature drop.

Summer 2015 was characterized by a severe heatwave and drought that lasted about a month between late-June and mid-July. Temperatures were 5 to 7 °C higher than average for two consecutive weeks, making this period the warmest on record. Between the end of July and the debris flow event (August 14^{th}), a series of rainfall events with intensities ranging from 10 to 35 mm/day were recorded, for a total amount of 220 mm of precipitation. Compared to previous years, the three-week period previous to the 2015 debris flow event represented the wettest on record to occur in summer.

In particular, the last days before the debris flow events were characterized by a series of relatively intense precipitations. The second-strongest precipitation event of the year (35 mm/day) occurred on August 8^{th}, followed the next day by a smaller event (15 mm/day). After three days without precipitation, 10 mm of rain were recorded on August 13^{th} at the Mont Cenis station and finally an event of precipitation of about 30 mm/day characterized the day of the events (August 14^{th}). None of these precipitation events were exceptional in terms of intensity as rainy events above 60 mm/day and up to 90 mm/day were regularly recorded at the Mont Cenis station since 1992.

4.2 Landform dynamics

4.2.1 Historical aerial imagery

The Lou rock glacier has experienced a generalized acceleration over the past four decades (Figure 6). The western lobe systematically showed the highest velocities of the whole landform, with velocities increasing from 0.5 ± 0.1 m/y (1970 – 1996) to $1.0/pm0.2$ m/y (1996 -2006), then to $1.9/pm0.2$ m/y (2006 – 2013) to finally reach $3.5/pm0.3$ m/y (2013 – 2017). The eastern lobe exhibited similar behaviour with velocity gradually increasing from 0.15 m/y (1970 – 1996) to 1.3 m/y (2013 -2017), while the central lobe apparently encountered a less pronounced acceleration (0.3 m/y in 1996 – 2006 to 0.6 in 2013 – 2017). The inactive lobes on the western side appeared to have experienced a strong reactivation between 2006-2013, as the velocity increased from 0.3 m/y (1996 -2006) to 1.3 m/y (2006 – 2013) with substantial observable frontal advance (Figure 7). Since 2013, these lobes have remained almost inactive, as velocity dropped down to about 0.2 m/y (2013 – 2017). A significant frontal advance of about 20 meters could also be observed for the western lobe between 2006 and 2017 (Figure 7). Depending on image pairs, the image distortion uncertainty estimated by observing stable areas was evaluated to be of the order of 0.1 to 0.3 m/y, and thus in most cases significantly lower than the surface velocity values. The calculated displacement rates and their variability can therefore be considered reliable.

4.2.2 dGPS

DGPS measurements were conducted only on the western lobe and only two targets could be measured continuously from 2015 to 2018. Displacement data indicated a slight deceleration in 2016-2017 compared to 2015-2016 and an acceleration between 2016-2017 and 2017-2018, reaching displacement rates about 10% higher than the period 2015-2016. Measurements indicated that the frontal part moved faster (about 3.5 m/y) than the rest of the lobe, with the lowest values of surface velocity measured at the limit between the western and the central lobes.

4.2.3 UAV photogrammetry

Velocity values extracted from UAV photogrammetry were considered significant above 0.53 m/y, as apparent movements on stable areas were observable only below this threshold. The comparison between UAV-derived orthoimages allowed surface displacements at a high spatial resolution to be identified and highlighted the complex morphology and heterogeneous creeping patterns of the rock glacier complex. The western lobe moved significantly faster than the other lobes between 2017 and 2018 (Figure 8). The highest velocities (<3.5 m/y) were observed close to the edge of the front and in the western part of the lobe (Figure 8). Comparison between displacement values obtained from the UAV surveys and from dGPS in this area for the same period showed good correlation (Figure 8). The eastern lobe was found to creep at about 1 to 1.5 m/y, showing also maximum velocities at its front. This lobe seems to diverge into two minor lobes moving in two different directions, possibly due to the underlying bedrock topography. On the slope above the eastern plateau, it was possible to see a system of small fast-moving lobes creeping at rates of 2.5 m/y. A similar pattern is observable upslope of the central plateau, where a minor lobe is creeping downslope at a velocity of 1.5 m/y while the rest of the area shows only small movements (below the limit of detection). Finally, it was possible to identify two small surface slides on the front of the central lobe.

DEM subtraction showed a confidence interval, i.e. the double of the standard deviation of elevation changes on stable areas, of 0.48 m. This threshold was used as a lower limit of detection and surface variations below this value were discarded. The comparison of the DEMs obtained for 2016 and 2018 showed a significant debris accumulation on the lower part of the western lobe front, reaching 1.6 m thickness and a total volume of about 1000 m^3 (Figure 9). The edge of the front does not seem to have significantly moved forward or backward between 2016 and 2018. The western slope failure did not evolve significantly since the event of 2015, with only minor accumulations observed below the main scarp.

4.3 Geophysical Investigations

4.3.1 ERT investigations

The PE1 profile revealed a high resistive body located in the centre of the eastern plateau (Figure 10a). Resistivity reached 3 000 kΩ in the depression, at about 20 meters depth. This resistive body was surrounded by more conductive terrains, ranging between 10 – 50 kΩ. The upper part of the central plateau showed the presence of a resistive body reaching 500 kΩ at 10 – 15 meters depth and located in the middle of the central lobe. It was possible to observe lower resistivity (20 – 40 kΩ) in the zone of origin of the western lobe (Profile PE2).

Resistivity was generally lower in the western sector. The longitudinal profile on the western lobe (PE5) ranged from 0.5 kΩ downslope up to 500 kΩ upslope. Starting upward from the front line, a resistive body could be observed at 20 meters depth, with resistivity values ranging from about 10 – 30 kΩ in the downslope part and up to 500 kΩ on the upslope part of the profile. Below the resistive body, values dropped quickly to 2 – 0.5 kΩ, reaching similar values to those that can be observed downstream from the front in areas believed to be free from permafrost.

The transversal profile across the debris flow slope failures (PE6) showed resistivity values generally ranging from 0.5 to 10 kΩ, except for a small resistive body identified at about 20 m deep in the middle of the profile and corresponding to the terminal part of the western lobe. Lower resistivity values ranging from 1 to 5 kΩ were found all long the profile at 20 to 30 meters depth.

4.3.2 Seismic refraction investigations

The seismic profile PS3 reached a depth of 17 m in the downslope half and 30 meters in the upslope half (Figure 10b). Wave velocities ranged from 300 to 5000 m/s. Higher velocities could be found upslope, near the limit between the western and the central lobes. Lower velocities were observed in isolated surface patches and down to about 2 – 5 m in depth. In general, wave velocity increased linearly with depth. In the downslope part of the profile, wave velocity increased from 500 to 4000 m/s within 15 m depth. In the central section the velocity increase rate was gentler, as velocity ranged from 1000 to 3000 m/s at 30 meters depth. The velocity strongly increased upslope, within 10-15 meters from 300 to 5000 m/s.

5 Discussion

5.1 Historical and Recent dynamics

5.1.1 Results Interpretation

A marked acceleration was found to characterize the Lour rock glacier during the past decades, consistent with several other rock glaciers in the European Alps[41,42]. The rate of the acceleration on the western lobe over the past four decades (from 0.8 in the period 1970-1996 to 3.6 m/y in the period 2013-2017, i.e. + 400%) can be compared to other cases of rapidly moving rock glaciers[9,10,12,43,44] and suggests a partial destabilization of the landform. UAV and dGPS surveys confirmed the high current velocity of the western lobe, especially in its frontal zone where velocity rates reached about 3.7 m/y between 2017 and 2018. According to the crack development process described by previous studies[12,15,45], pebbly rock glaciers characterized by temperate permafrost conditions and extensive flow patterns are highly susceptible to cracking due to the tension generated on the landform surface. This is the case for the western lobe, where displacement rates are about three times higher at the front than the areas close to the rooting zone and where most of the cracks are observable. Cracks generate preferential water flow paths in the landform that encourage reduction of the shear stress resistance and increase the heat transfer by advection. As a consequence, positive feedback processes can be triggered and lead to a further increase in permafrost creep rates, permafrost temperatures and even encourage development of new cracks.

5.1.2 Limitations of the method

Most of the uncertainties associated with the assessment of the rock glacier dynamics were related to the historical analysis. The rock glacier is relatively small in size and its location on steep slopes may induce critical distortions in the computation of orthomosaics from historical images. Stable areas used to assess the errors were often located in zones characterized by flatter slopes in comparison to the rock glacier surface and the calculated uncertainties may be under-estimated in steeper areas. These errors can be illustrated by the change in direction of displacement vectors between consecutive time intervals, which sometimes exceeded 40 degrees of aspect change. Despite limitations, GPS and UAV data confirmed the order of magnitude of the movements observed on the last image pair (2013-2017) and seem to highlight the validity of the values obtained from the analysis of old aerial images.

5.2 Internal structure

5.2.1 ERT profiles

The highly resistive body measured at the eastern plateau (PE1) indicates the presence of massive ice, which is also supported by the probably glaciogenic formation of this lobe. The depression observed in this area may thus be caused by the partial thaw of this ice body. The geoelectric profile suggested a massive ice thickness of about 15 meters, with some uncertainty due to the limited depth of the investigation rendering the identification of a clear transition between the highly resistive massive ice and a potentially underlying more conductive body impossible (bedrock or unfrozen sediments).

Lower values of resistivity were measured on the western lobe. They are typical for temperate permafrost with low ice

content and fine-grained sedimentary material[46] and suggest a periglacial genesis of this area of the landform[47]. The resistive body observed in the profiles PE1 and PE2 appeared to be 20 meters deep and about 50 meters wide, showing increasing values of resistivity upslope. The presence of temperate permafrost on the western lobe is in agreement with the development of high displacement rates and surface cracking[12,15].

5.2.2 SRT profiles

The seismic profile provided relevant information on the internal structure of the western lobe. Penetration of the waves was limited in depth to around 20 – 30 meters. This depth correlated with the transition between high and low resistivity values observed in the ERT. This transition probably corresponds to a reduction in ice content, and indicates that the western lobe creeps above a layer of unfrozen sediments or densely jointed bedrock. However, a better characterization of the material present under the permafrost body would require further investigations including for instance a deeper sounding.

In addition, the lower seismic velocity values observed near the surface suggested an active layer depth of 2-3 meters on the western lobe. An apparent increase in active layer thickness can be identified in the medial part of the lobe on the seismic profile, reaching up to 5 meters in depth. In this area, the velocity anomalies seem to be correlated with the presence of cracks and may be induced by higher air content at shallow depth. The presence of these disturbances up to a depth of 5 m, i.e. deeper than the estimated active layer thickness (2-3 m) indicates that the cracks propagate in the upper part of the permafrost body.

5.3 A comprehensive diagnosis of the frontal failures

Both the geomorphological characteristics and the presence of water springing out of the head scarps indicate that the frontal slope failures resulted from intense linear regressive erosion, previously described as concentrated flow processes from observations conducted at Dirru, Gugla and Tsarmine rock glaciers in the western Swiss Alps[1]. In order to describe and explain in detail the occurrence of this process in the case of the Lou rock glacier, we subdivided the discussion into three parts: the local predispositions, the meteorological conditions prior to the event and then the triggering factors.

5.3.1 Predisposition : Topographical and geomorphological characteristics of the rock glacier

The Lou rock glacier developed on a flat ledge located in an otherwise very steep topographical setting. The front of the rock glacier is very steep (up to 42°) and directly connected to torrential gullies. The general topographical setting of the area thus encourages the occurrence and propagation of erosion and sediment transfer processes by gravity[1].

The eastern slope failure occurred at the limit between the central and the eastern fronts where traces of previous events (head scarps and gullies) were in evidence on historical imagery dating back to 1953 (Figure 7). Therefore, the concentrated flow process causing the 2015 eastern failure had most likely already occurred in the past decades. In addition to the steep front directly connected to the gully system, the presence of a topographical depression located upslope from the head scarp and characterized by the presence of massive ice only a few decimetres below the surface is expected to encourage water concentration and circulation on top of the ice body and lead to frequent release of water onto the frontal slope where the failure was observed. As a result, concentrated water flow can be generated and lead to intense regressive erosion phases, similar to

those observed in the western Swiss Alps[1].

The western failure, on the other hand, represented a novel event as there were no indications of previous substantial erosion on the historical aerial images. Therefore, one can assume that the occurrence of the 2015 erosional event was either related to recent changes in the internal structure and morphological characteristics of the landform, or due to exceptional weather conditions, or both. The investigations conducted on the western lobe revealed relevant geomorphological modifications in the past decades that were related to the significant increase in velocity for the landform. These geomorphological modifications consisted of a significant advance of the front position and the development of cracks on the surface of the lobe. The observed progression of the front-line appears to have enhanced the connectivity between the rock glacier and the torrential system, since the 2015 failure occurred in an area occupied by the rock glacier only after 2006 (Figure 7). In addition, surface cracking is suspected to have reduced material shear resistance and increased the susceptibility to water infiltration upslope from the front-line[15], possibly enhancing the occurrence of supra-permafrost flow. In this sense, we suggest that the high displacement rates of the rock glacier and consequent destabilization process represent relevant changes that tended to increase the predisposition of the western lobe to failure. Permafrost thermal characteristics and internal structure also played a role in the occurrence of this process as rock glacier cracking and destabilization is known to be more likely to occur in temperate permafrost conditions[12, 15].

5.3.2 Preparation: meteorological conditions prior to the event

The meteorological sequence that preceded the failure events was characterized by several anomalies consisting of (i) scarce snow cover with an early snow disappearance at the end of the winter, (ii) the warmest heat wave on record between mid-June and mid-July and (iii) the wettest three-week period recorded in summer since 1992. All these factors are known to influence permafrost characteristics and slope stability but, due to the lack of in-situ data, the respective effects of these anomalies on the occurrence of the failures cannot be demonstrated by evidence. Nevertheless, we propose here a brief description of the processes that may have contributed to facilitation occurrence of the failures.

On the one hand, heat waves may lead to significant ground warming resulting in permafrost degradation and active layer thickening. The loss of permafrost ice content due to thawing and the increase of liquid water content associated with permafrost degradation[48] are often addressed as factors favouring the occurrence of mass movements in mountain environments due to the decrease of the frozen ground stiffness and resistance to shear stress[14]. This effect can be amplified with an early disappearance of the snow cover which leads to a longer period of ground exposure to solar radiation. In the case of the Lou rock glacier, the absence of data characterizing the thermal state of permafrost and the evolution of the active layer thickness prior to the event does not allow the role of these drivers to be identified as preparatory factors to the debris flow event.

On the other hand, repeated rainfalls are known to be an important factor influencing slope stability by reducing the shear stress resistance[12]. Progressive increase of the water content was for instance observed to be a relevant preparatory factor in the occurrence of frontal slope failures at the Dirru, Gugla and Tsarmine rock glaciers in the western Swiss Alps[1]. We can thus assume that the high total precipitation recorded during the weeks preceding the events had a large role to play in triggering the

Lou slope failures.

5.3.3 Trigger: concentrated flow consecutive to repeated rainfalls

The three weeks prior to the debris flows were characterized by a repetition of rainfall events of small to medium intensity. The frontal failures were ultimately triggered during a minor precipitation event. It appears that the significant infiltration of meteoric water resulting from the frequent rainy episodes led to saturation of the active layer and generated supra-permafrost flow. Water running on top of the permafrost table was still observable the day after the event at the head of the two failures and confirms the (almost) absence of infiltration within or below the permafrost body. Both western and eastern slope failures were then triggered by concentrated flow ([1]) that generated regressive erosion from two water springs located respectively at the outflow of the central plateau and the flat eastern plateau, which collects water from the nearby slopes.

The peculiar morphology of the western slide indicates that parts of the erosion occurred in one single sliding event. Such an event could have been triggered by the removal of sediment further downslope from linear flow erosion, diminishing the support for the debris lying at the front. A large-scale debris slide of this type could be the signature of large concentrated flow events on steep pebbly rock glacier fronts for which the higher ratio of finer grained sediments in comparison to blocky rock glaciers favours single slides instead of gradual rock falls.

5.4 Recommendations

Although the Lou frontal failures consisted of a volume only slightly more than 1000 m^3, the debris flow generated was able to mobilize up to 15 000 m^3 of debris stored in the Arcelle Neuve stream or on the sides of the torrential channel. The existing river infrastructures in this Alpine catchment were inadequate to face this event, which resulted in the flooding of th town of Lanslevillard. In order to mitigate the risk linked to possible future debris flow in the Arcelle Neuve stream, the RTM built a new protection infrastructure at the junction with the Arc River[49]. This infrastructure consists of an open channel which substitutes the former underground pipe in order to allow debris flows to continue and reach the Arc River where sediments will be evacuated by the main river flow. This channel was designed to be operational for debris flows up to 25 000 m^3. The volume was evaluated assuming future frontal failures of the same order of magnitude as the 2015 event in terms of mobilized materials and is consistent with other studies documenting similar debris flow mechanisms[1,8].

Due to its particularities, i.e. its direct connection with torrential channels and displacement patterns, we recommend that the Lou rock glacier should become a future reference site for permafrost research in the region. Annual monitoring involving repeated UAV photogrammetric surveys have been proven to be efficient to monitor both the evolution of the surface velocities and morphological changes characterizing the lobe fronts. Further efforts should focus on analysing the erosion processes at the front of the landform and the sediment transfer rate between the front and the gullies, in order to quantify the role of the rock glacier in the sediment chain. We propose an approach based on fixed camera monitoring[1,50] and high-resolution DEM difference of the upper and lower gully[13]. Furthermore, borehole investigations could bring significant information about the current state and evolution of the active layer depth, as well as the sedimentary properties of the western lobe. Finally, further efforts should focus on the characterization of other sediment sources and channel recharge rates in the lower sectors of the

Arcelle Neuve torrent to better establish debris flow scenarios.

6 Conclusions

In this study we provided a description of the frontal slope failures at the Lou rock glacier. While the characteristics of the eastern slide are typical of linear regressive erosion from concentrated water flow, the western slide presented geomorphological characteristics that resemble an active layer detachment (ALD), i.e. a slide of a portion of the active layer, mainly observed in Arctic permafrost sites. The development of this type of failure, and at such as scale, is probably due to the high ratio of fine-grained material characterizing the Lou rock glacier and which is more conducive to the occurrence of debris slides than individual or cascading rock falls that are commonly observed on boulder rock glacier fronts. In addition, the erosion observed during the 2015 events at the fronts of the Lou rock glacier only mobilized sediments within the active layer, corresponding to similar events observed at other rock glacier sites.

Both local topography (steep slopes) and the morphological settings (steep fronts overhanging gullies) of the landform are considered to be important factors preconditioning the occurrence of the slope failures. It has been possible to see the eastern failure in orthoimages since the 1950's, indicating that similar events occurred in the past. The western slide corresponds to the first event recorded in that sector since at least 1953 (oldest useable aerial image). In addition to the exceptionally wet conditions in the few weeks previous to the event, the recent increase in creep velocity leading to destabilization of the western lobe represents the most relevant changes that potentially explain the sudden occurrence of intense erosion in this sector. The destabilization of the western lobe is believed to have facilitated the development of a frontal slope failure (i) by reducing the distance between the frontal slope and the torrential gully, thus enhancing the rock glacier – torrent connectivity and (ii) by leading to the formation of tension cracks on the surface of the lobe, which favours the infiltration of water into the ground and leads to the occurrence of the concentrated flow process that triggered the debris flow events. In this sense, we suggest that rock glacier destabilization may have a significant impact on on-site predisposition to failure. However, further investigations would be needed in order to provide better evidence for the effects of such destabilizations on the sediment transfer activity between rock glacier fronts and torrents.

Moreover, we highlighted here the anomalous 2014-2015 meteorological conditions, characterized by scarce snow cover in late winter, the occurrence of a strong heat wave between late June and mid-July and an exceptionally wet period in the few weeks preceding the failures. The debris flows occurred after a series of meteoric water inputs, pointing out the important role of water availability on triggering such intense erosion events. In addition, it is emphasized that rainy events were not exceptionally intense but occurred regularly over a three-week period, suggesting that the frequency of precipitation events was critical in triggering the failure, as opposed to their intensity. It has been mentioned that the western slope failure was a novel event and had probably been preconditioned by the recent destabilization of the corresponding lobe. It is also important to acknowledge the exceptional character of the precipitation patterns prior to the event as another explanatory factor for the occurrence of such unprecedented events. If the direct impact of the weather conditions on the landform could not be analyzed

in detail due to data scarcity, we point out that the correlation between meteorological anomaly and failure events would merit further research effort in the future in order to improve understanding of the link between climate and the thermal state of the rock glacier.

References

1. M. Kummert, R. Delaloye, and L. Braillard. Erosion and sediment transfer processes at the front of rapidly moving rock glaciers: Systematic observations with automatic cameras in the western Swiss Alps. *Permafrost and Periglacial Processes*, 29(1):1–13, 2017.

2. C. Huscroft, P. S. Lipovsky, and J. D. Bond. Permafrost and landslide activity: Case studies from southwestern Yukon Territory. *Yukon Exploration and Geology 2003*, pages 107–119, 2004.

3. A.G. Lewkowicz. Morphology, frequency and magnitude of active layer detachment slides, Fosheim Peninsula, Ellesmere Island, NWT. *Permafrost-Canada, Proceedings of the Fifth Canadian Permaf rost Conference: Université Laval, Nordicana*, pages 111–118, 1990.

4. A. G. Lewkowicz and C. Harris. Frequency and Magnitude of Active-layer Detachment Failures in Discontinuous and Continuous Permafrost, Northern Canada. *Geomorphology*, 69(1-4):275–297, 2005.

5. S. M. Springman, Y. Yamamoto, T. Buchli, M. Hertich, H. Maurer, K. Merz, I. Gärtner-Roer, and L. Seward. Rock Glacier Degradation and Instabilities in the European Alps: A Characterisation and Monitoring Experiment in the Turtmanntal, CH. *Landslide Science and Practice*, 4(June):329–333, 2013.

6. W Haeberli, Y Schaub, and C Huggel. Increasing risks related to landslides from degrading permafrost into new lakes in de-glaciating mountain ranges. *Geomorphology*, 293(February):405–417, 2017.

7. Mario Kummert and Reynald Delaloye. Regional-scale inventory of periglacial moving landforms connected to the torrential network system. *Geograp*, 73:357–371, 2018.

8. R Lugon and M Stoffel. Rock-glacier dynamics and magnitude-frequency relations of debris flows in a high-elevation watershed: Ritigraben, Swiss Alps. *Global and Planetary Change*, 73(3-4):202–210, 2010.

9. R. Delaloye, S. Morard, C. Barboux, D. Abbet, V. Gruber, M. Riedo, and S. Gachet. Rapidly moving rock glaciers in Mattertal. *Jahrestagung der Schweizerischen Geomorphologischen Gesellschaft*, (29):21–31, 2013.

10. I. Roer, W. Haeberli, M. Avian, V. Kaufmann, R. Delaloye, C. Lambiel, and A. Kääb. Observations and considerations on destabilizing active rock glaciers in the European Alps. In *Proceedings of the 9th International Conference of Permafrost, Fairbanks, Alaska*, number 4, pages 1505–1510, 2008.

11. M. Marcer, C. Serrano, A. Brenning, X. Bodin, J. Goetz, and P. Schoeneich. Evaluating the destabilization susceptibility of active rock glaciers in the French Alps. *The Cryosphere*, 13:141–155, 2019.

12. T. Buchli, A. Kos, P. Limpach, K. Merz, X. Zhou, and S. M. Springman. Kinematic investigations on the Furggwanghorn Rock Glacier , Switzerland. *Permafrost and Periglacial Processes*, 29(3):3–20, 2018.

13. M. Kummert and R. Delaloye. Mapping and quantifying sediment transfer between the front of rapidly moving rock glaciers and torrential gullies. *Geomorphology*, 309:60–76, 2018.

14. M. C. R. Davies, O. Hamza, and C. Harris. The Effect of Rise in Mean Annual Temperature on the Stability of Rock Slopes Containing Ice-Filled Discontinuities. *Permafrost and Periglacial Processes*, 12(November 2001):137–144, 2001.

15. Y. Yamamoto and S. M. Springman. Three- and four-point bending tests on artificial frozen soil samples at temperatures close to 0 C. *Cold Regions Science and Technology*, 134(C):20–32, 2017.

16. C. Huggel, N. Salzmann, S. Allen, J. Caplan-Auerbach, L. Fischer, W. Haeberli, C. Larsen, D. Schneider, and R. Wessels. Recent and future warm extreme events and high-mountain slope stability. *Philosophical Transactions of the Royal Society A: Mathematical, Physical and Engineering Sciences*, 368(1919):2435–2459, 2010.

17. X. Bodin, J. M. Krysiecki, P. Schoeneich, O. Le Roux, L. Lorier, T. Echelard, M. Peyron, and A. Walpersdorf. The 2006 Collapse of the Bérard Rock Glacier (Southern French Alps). *Permafrost and Periglacial Processes*, 28(1):209–223, 2016.

18. S Fudral, E Deville, G Nicoud, U Pognate, P L Guillot, and E Jaillard. *Notice explicative de la feuille Lanslebourg-Mont-d'Ambin à 1/50000*. 1994.

19. F. Gottardi. *Estimation statistique et réanalyse des précipitations en montagne Utilisation d'ébauches par types de temps et assimilation de données d'enneigement Application aux grands massifs montagneux français*. PhD thesis, Institut National Polytechnique de Grenoble - INPG, 2009.

20. Y. Durand, G. Giraud, M. Laternser, P. Etchevers, L. Mérindol, and B. Lesaffre. Reanalysis of 47 years of climate in the French Alps (1958-2005): Climatology and trends for snow cover. *Journal of Applied Meteorology and Climatology*, 48(12):2487–2512, 2009.

21. M. Gardent. *Inventaire et retrait des glaciers dans les Alpes françaises depuis la fin du Petit Age Glaciaire*. PhD thesis, Université Savoie, EDYTEM, France, 2014.

22. M. Marcer, X. Bodin, A. Brenning, P. Schoeneich, R. Charvet, and F. Gottardi. Permafrost Favorability Index: Spatial Modeling in the French Alps Using a Rock Glacier Inventory. *Frontiers in Earth Science*, 5(December):1–17, 2017.

23. S. Monnier. *Les glaciers-rocheux, objets géographiques*. PhD thesis, Université Paris XIII, Laboratoire de Géographie Physique EA, France, 2006.

24. A. Ikeda and N. Matsuoka. Pebbly versus bouldery rock glaciers: Morphology, structure and processes. *Geomorphology*, 73(3-4):279–296, 2006.

25. R. Frauenfelder and A. Kääb. Towards a palaeoclimatic model of rock-glacier formation in the Swiss Alps. *Annals of Glaciology*, 31(1):281–286, 2000.

26. A. Kääb, W. Haeberli, and G. H. Gudmundsson. Analysing the creep of mountain permafrost using high precision aerial photogrammetry: 25 years of monitoring Gruben rock glacier, Swiss Alps. *Permafrost and Periglacial Processes*, 8(4):409–426, 1997.

27. A. Kääb, V. Kaufmann, R. Ladstädter, and T. Eiken. Rock glacier dynamics : implications from high-resolution measurements of surface velocity fields. In S. Phillips, S. M. Springman, and L. Arenson, editors, *Permafrost*, pages 501–506. Swets & Zeitlinger, Lisse, 2003.

28. C. Lambiel and R. Delaloye. Contribution of real-time kinematic GPS in the study of creeping mountain permafrost: Examples from the Western Swiss Alps. *Permafrost and Periglacial Processes*, 15(3):229–241, 2004.

29. E. Dall'Asta, G. Forlani, R. Roncella, M. Santise, F. Diotri, and U. Morra di Cella. Unmanned Aerial Systems and DSM matching for rock glacier monitoring. *ISPRS Journal of Photogrammetry and Remote Sensing*, 127:102–114, 2017.

30. X. Bodin, E. Thibert, Olivier Sanchez, Antoine Rabatel, and Stéphane Jaillet. Multi-Annual Kinematics of an Active Rock Glacier Quantified from Very High-Resolution DEMs : An Application-Case in the French Alps. *Remote Sensing*, 10(4):547, 2018.

31. IGN. BD ALTI® Version 2.0 - Descriptif de contenu. Technical report, Institut national de l'information géographique et forestière, 2017.

32. M. W. Smith, J. L. Carrivick, and D. J. Quincey. Structure from motion photogrammetry in physical geography. *Progress in Physical Geography*, 40(2):247–275, 2016.

33. T A Scambos, M J Dutkiewic, C J Wilson, and R A Bindschadler. Application of image cross-correlation to the measurement of glacier velocity using satellite image data. *Remote Sensing of Environment*, 42(3):177–186, 1992.

34. P. J. Besl and N. D. McKay. A Method for Registration of 3-D Shapes. *IEEE Transactions on Pattern Analysis and Machine Intelligence*, 14(2):239–256, 1992.

35. D Girardeau-Montaut. *Détection de Changement sur des Données Géométriques Tridimensionnelles.* PhD thesis, 2006.

36. H. Maurer and C. Hauck. Instruments and methods: Geophysical imaging of alpine rock glaciers. *Journal of Glaciology*, 53(180):110–120, 2007.

37. C. Kneisel, C. Hauck, R. Fortier, and B. Moorman. Advances in Geophysical Methods for Permafrost Investigations. *Permafrost and Periglacial Processes*, 19:157–178, 2008.

38. D. Draebing. Application of refraction seismics in alpine permafrost studies: A review. *Earth-Science Reviews*, 155:136–152, 2016.

39. M H Loke and R D Barker. Rapid least-squares inversion of apparent resistivity pseudosections by a quasi-Newton method. *Geophysical Prospecting*, 44:131–152, 1996.

562 **40.** OBSCAN. Le Changement Climatique dans les alpes du Nord - Enneigement 2014 - 2015. *Academie Francaise*, pages
563 1–21, 2015.

564 **41.** R. Delaloye, E. Perruchoud, M. Avian, Vi. Kaufmann, X. Bodin, H. Hausmann, A. Ikeda, A. Kääb, A. Kellerer-Pirklbauer,
565 K. Krainer, C. Lambiel, D. Mihajlovic, B. Staub, I. Roer, and E. Thibert. Recent Interannual Variations of Rock Glacier
566 Creep in the European Alps. In *Proceeding of the Ninth International Conference on Permafrost*, pages 343–348, Fairbanks,
567 Alaska, 2008.

568 **42.** A Kellerer-Pirklbauer, R Delaloye, C Lambiel, I Gärtner-Roer, V Kaufmann, C Scapozza, K Krainer, B Staub, E Thibert,
569 X. Bodin, A Fischer, L. Hartl, U Morra di Cella, V Mair, M Marcer, and P Schoeneich. Interannual variability of rock
570 glacier flow velocities in the European Alps. In *Proceedings of the 5th European Conference on Permafrost*, pages 396–397,
571 Chamonix, France, 2018.

572 **43.** R Scotti, G B Crosta, and A Villa. Destabilisation of Creeping Permafrost: The Plator Rock Glacier Case Study (Central
573 Italian Alps). *Permafrost and Periglacial Processes*, 28(1):224–236, 2016.

574 **44.** H. Ø. Eriksen, L. Rouyet, T. R. Lauknes, I. Berthling, K. Isaksen, H. Hindberg, Y. Larsen, and G. D. Corner. Recent
575 Acceleration of a Rock Glacier Complex , Ádjet , Norway , Documented by 62 Years of Remote Sensing Observations.
576 *Geophysical Research Letters*, 45, 2018.

577 **45.** A. Ikeda, N. Matsuoka, and A. Kääb. Fast deformation of perennially frozen debris in a warm rock glacier in the Swiss
578 Alps: An effect of liquid water. *Journal of Geophysical Research: Earth Surface*, 113(1):1–12, 2008.

579 **46.** A Ikeda. Combination of conventional geophysical methods for sounding the composition of rock glaciers in the Swiss
580 Alps. *Permafrost and Periglacial Processes*, 17(1):35–48, 2006.

581 **47.** C. Hauck. Frozen ground monitoring using DC resistivity tomography. *Geophysical Research Letters*, 29(21):2016, 2002.

582 **48.** C. Huggel, J.J. Clague, and O. Korup. Is climate change responsible for changing landslide activity in high mountains?
583 *Earth Surface Processes and Landforms*, 37(1):77–91, 2012.

584 **49.** RTM. Etude hydraulique et propositions d ' aménagements pour la protection contre les débordements de l ' Arcelle Neuve.
585 Technical report, Service Département RTM de la Savoie, 42, Quai Charles Roissard 73026 Chambéry Cédex, 2016.

586 **50.** G Marsy, F Vernier, X Bodin, W Castaings, and E Trouvé. Détection automatique de zones en mouvement dans des
587 séries d ' images non recalées : Application à la surveillance des mouvements gravitaires Calcul du champ de vecteurs dé-
588 placement et segmentation Calcul du champ de déplacement. *Revue Française de Photogrammétrie et de Télédétection*, 8,
589 2018.

590 Acknowledgements

591 The present study was funded by the region Auvergne-Rhone Alpes through the ARC-3 grant and by the European Regional
592 Development Fund (POIA PA0004100) grant. The Lanslebourg - Val Cenis municipality also contributed to the present study

593 by funding internships within the PERMARISK project.

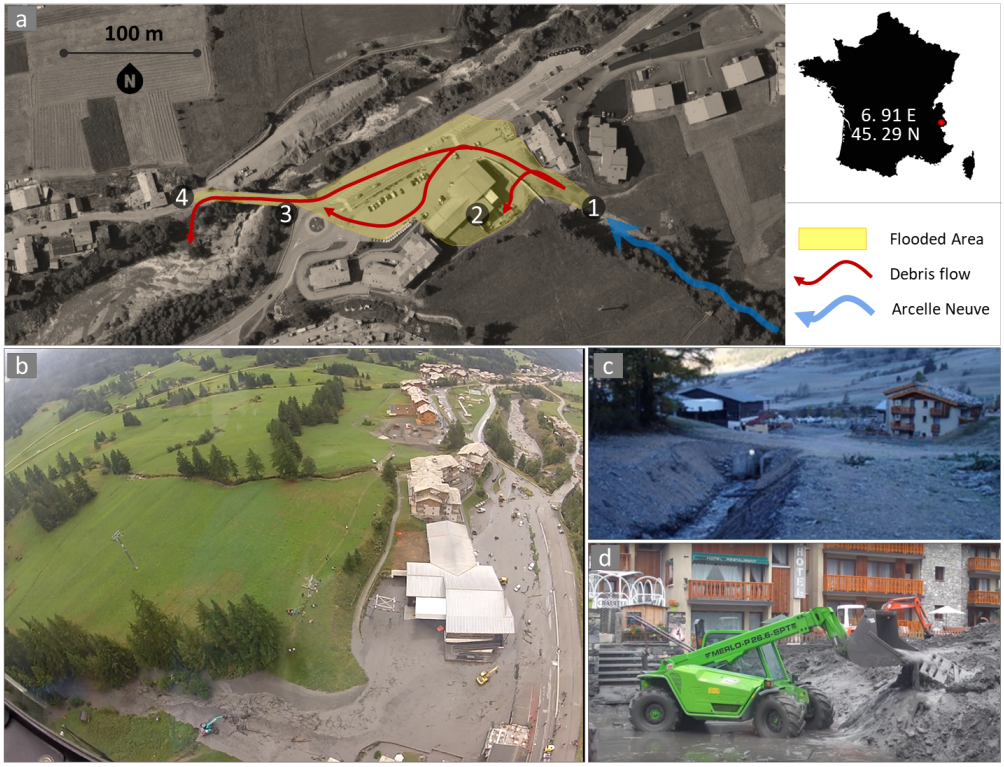

Figure 1. Overview of the debris flow that flooded the town of Lanslevillard the 14^{th} August 2015. On top left (panel a) it is shown (1) the debris flow transiting in the Arcelle Neuve stream, which passes through a narrow pipe under the town (panel c). (2) The pipe got jammed and the debris started to flood the departmental road D902 and buildings nearby (panel b and d). (3) The flow took a secondary road towards the inhabited centre of "Les Champs". (4) The flow was finally deviated into the Arc river by setting up an emergency embankment

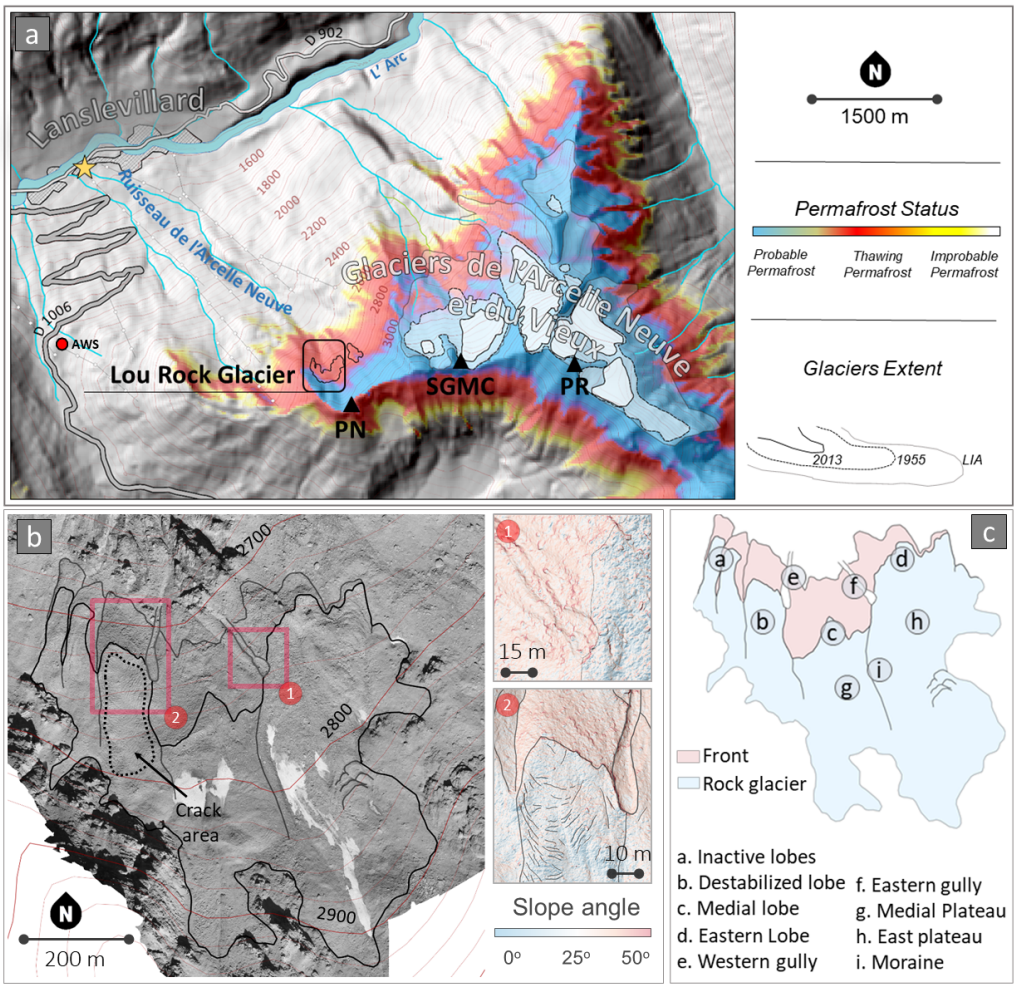

Figure 2. Overview of the Lou rock glacier. In panel a is presented the cryosphere status in the Mont Cenis Range. Glacier data[21] and permafrost status[11]. Acronyms: PN: Pointe de la Nunda; PR: Pointe de Ronce; SGMC: Signal du Grand Mont Cenis; AWS: Automatic Weather Station of Mont Cenis. In panel b is presented a high resolution orthoimage of the rock glacier obtained by UAV photogrammetry the 14th September 2016. In panel c is presented toponomy used in the present study to address the structure of the landform.

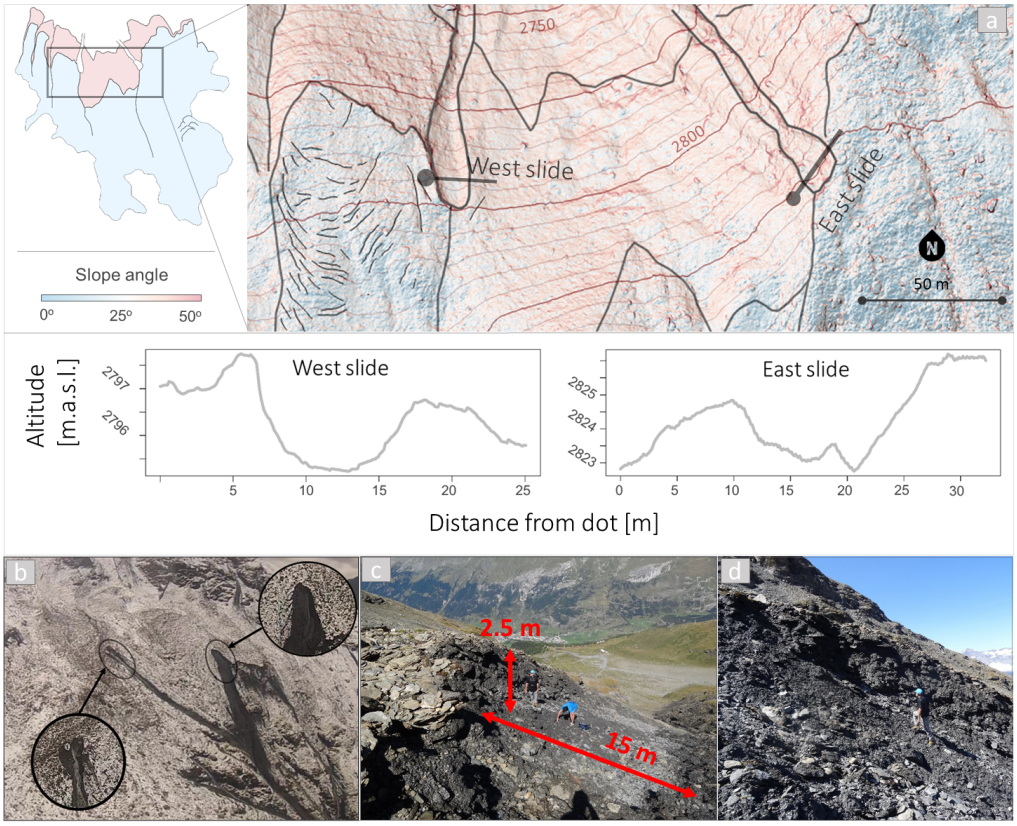

Figure 3. Overview of the frontal slopes failures. On top (panel a) are presented the morphometric characteristics of the two gullies. High resolution altitude, slope and hillshade data were obtained by UAV photogrammetry on September 14th 2016. On bottom left (panel b) is shown an aerial view of the failures taken the day after the event. On centre and right (panels c and d) is shown the west gully, characterizes by flat smooth surface and steep lateral embankments.

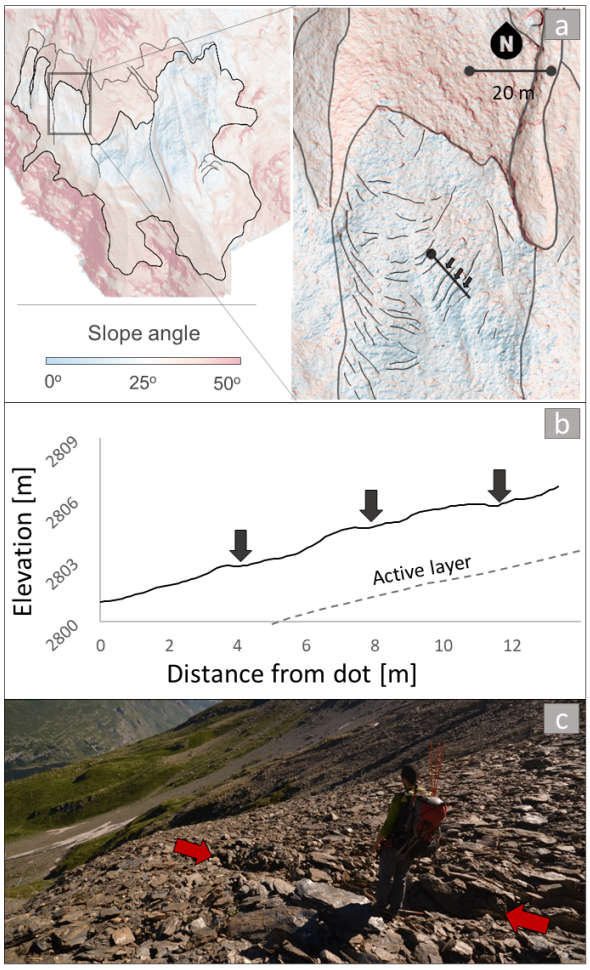

Figure 4. Example of cracks on the western lobe. The cracks are identified by the black arrows in the map (panel a) and on the topographical profile (b). Active layer depth is retrieved from seismic refraction, see section 4.3.2. On panel c is presented the appearance of one crack as it can be observed on the field.

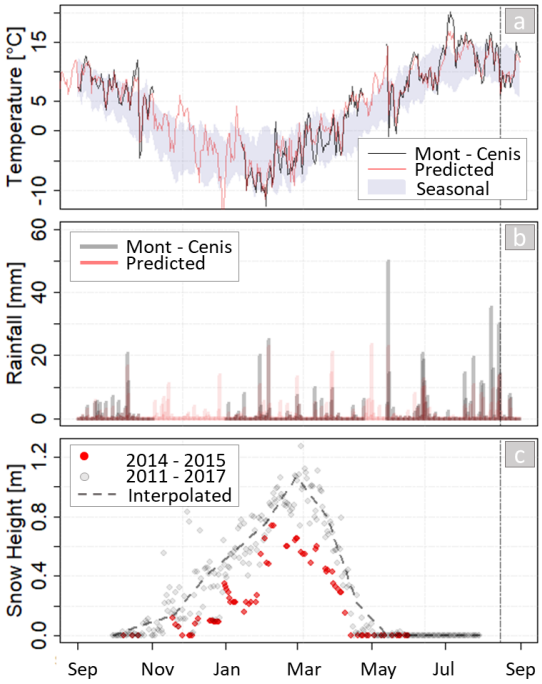

Figure 5. Overview of meteorological and nivological conditions in 2014-2015 prior to the failure event. Temperature and precipitation data (panels a and b) belong to Mont Cenis weather station. Data from Bessans weather station were used to fill gaps in the data set. Nivological data (panel c) belong to Bessans weather station and are compared to data between 2011 and 2017 to observe the 2014-2015 winter anomaly. Data are not continuous as manually observed every 1 to 5 days. Interpolation between 2011-2017 was performed only for visual support.

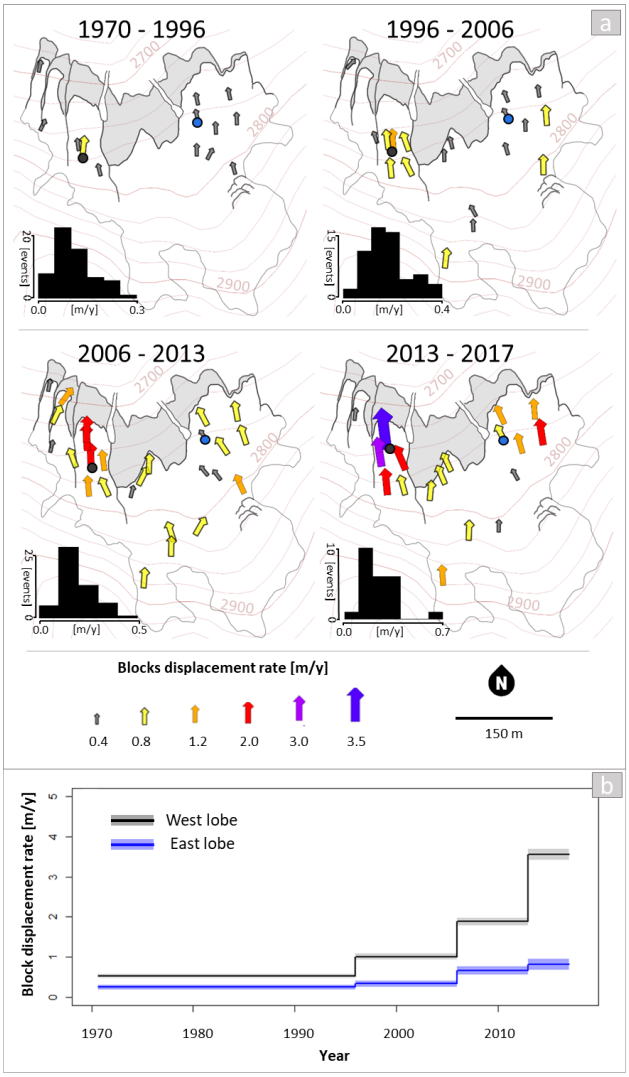

Figure 6. Overview of the historical dynamics of the Lou rock glacier presented as evolution of surface displacement rates retrieved by manual feature tracking on historical aerial imagery. For each displacement rates map are presented the frequency histograms of the relative movements in m/y measured on fixed areas between the orthoimage pairs. In panel b is presented the graph of the evolution of the displacement rate on two boulders, on for the western lobe and one for the eastern lobe. Shaded areas size represent the mean error evaluated by apparent movements on stable areas. Boulder locations is identified by a dot in the maps in panel a.

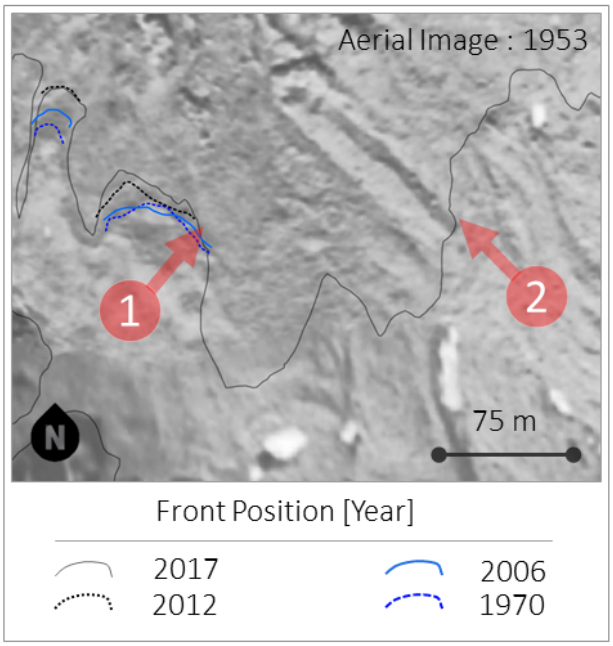

Figure 7. Overview of the advancement of the destabilized lobe front retrieved observable on historical aerial imagery.

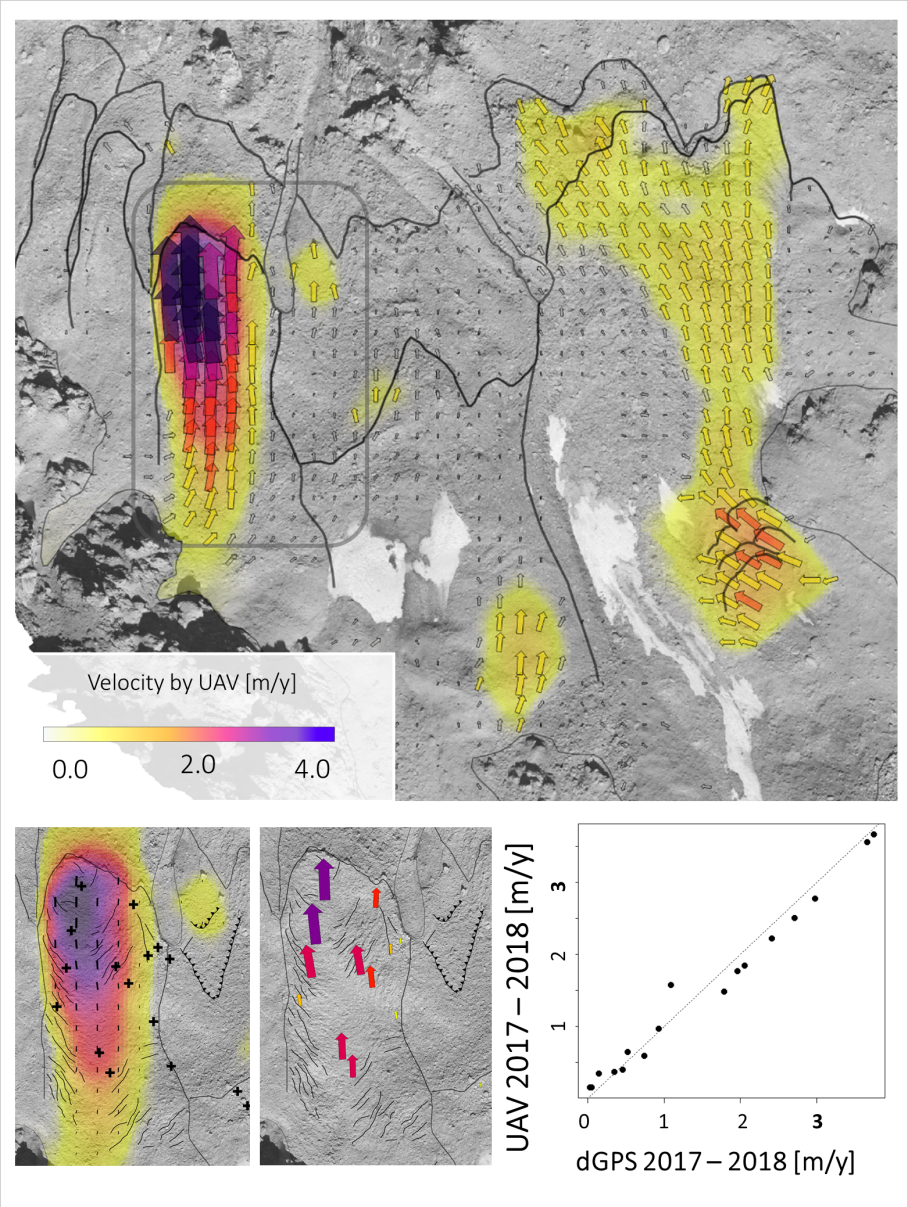

Figure 8. Overview of the dynamics of the rock glacier between 2017 and 2018. On top, measurements by UAV orthoimages comparison using automatic feature tracking in IMCORR. On bottom, comparison between UAV measurements and dGPS measurements.

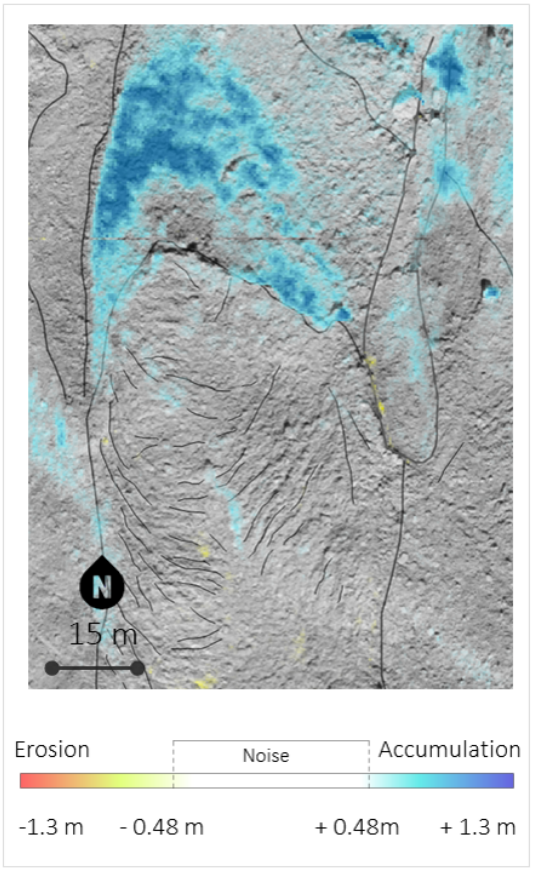

Figure 9. Surface variations at the front of the western lobe between 2016 and 2018 obtained by comparing high resolution UAV DEMs.

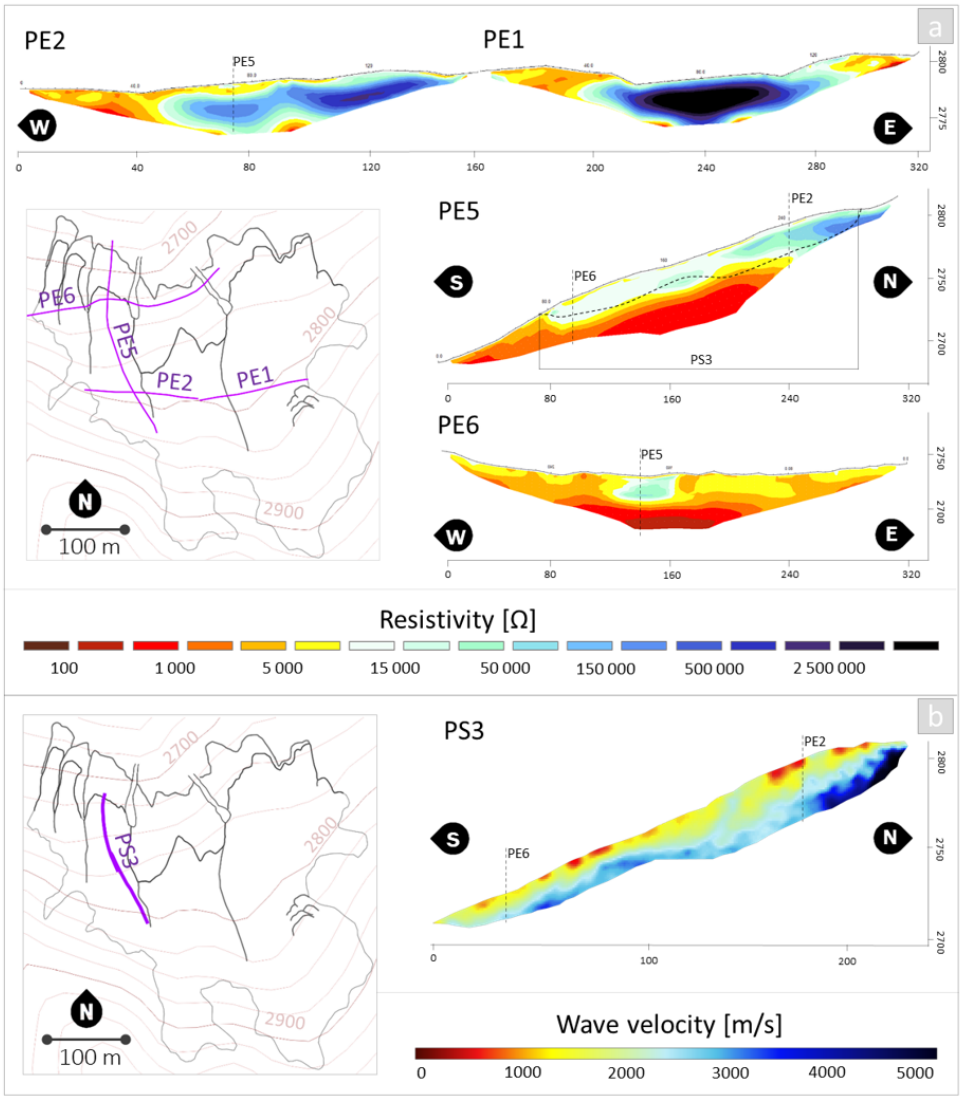

Figure 10. Overview of geophysical investigations at Lou rock glacier. On top (a), ERT transects acquired in 2016 (PE1 and PE2) and 2017 (PE5 and PE6). On bottom (b), SRT transect acquired in 2017.

Table 1. Summary of ERT transects.

	PE1	PE2	PE5	PE6
Dates of survey	15/09/2016	15/09/2016	10/08/2017	10/08/2017
Electrode array type	Wenner	Wenner	Wenner	Wenner
Electrode spacing	2.5 m	2.5 m	5 m	5 m
Number of electrodes	64	64	64	64
Number of data-points	651	650	456	472
Number of inverted points	646	647	452	459
Iterations	4	4	4	4
Absolute Error	5.4 %	6.3 %	5%	6%